

AD _____

GRANT NUMBER DAMD17-94-J-4301

TITLE: Sphingolipid-Mediated Apoptosis and Tumor Suppression in
Breast Carcinoma

PRINCIPAL INVESTIGATOR: Yusuf A. Hannun, M.D.

CONTRACTING ORGANIZATION: Duke University Medical Center
Durham, North Carolina 27710

REPORT DATE: October 1998

TYPE OF REPORT: Final

PREPARED FOR: Commander
U.S. Army Medical Research and Materiel Command
Fort Detrick, Frederick, Maryland 21702-5012

DISTRIBUTION STATEMENT: Approved for public release;
distribution unlimited

The views, opinions and/or findings contained in this report are those of the author(s) and should not be construed as an official Department of the Army position, policy or decision unless so designated by other documentation.

REPORT DOCUMENTATION PAGE

Form Approved

OMB No. 0704-0188

Public reporting burden for this collection of information is estimated to average 1 hour per response, including the time for reviewing instructions, searching existing data sources, gathering and maintaining the data needed, and completing and reviewing the collection of information. Send comments regarding this burden estimate or any other aspect of this collection of information, including suggestions for reducing this burden, to Washington Headquarters Services, Directorate for Information Operations and Reports, 1215 Jefferson Davis Highway, Suite 1204, Arlington, VA 22202-4302, and to the Office of Management and Budget, Paperwork Reduction Project (0704-0188), Washington, DC 20503.

1. AGENCY USE ONLY (Leave blank)		2. REPORT DATE October 1998	3. REPORT TYPE AND DATES COVERED Final (30 Sep 94 - 29 Sep 98)	
4. TITLE AND SUBTITLE Sphingolipid-Mediated Apoptosis and Tumor Suppression in Breast Carcinoma			5. FUNDING NUMBERS DAMD17-94-J-4301	
6. AUTHOR(S) Yusuf A. Hannun, M.D.				
7. PERFORMING ORGANIZATION NAME(S) AND ADDRESS(ES) Duke University Medical Center Durham, North Carolina 27710			8. PERFORMING ORGANIZATION REPORT NUMBER	
9. SPONSORING/MONITORING AGENCY NAME(S) AND ADDRESS(ES) Commander U.S. Army Medical Research and Materiel Command Fort Detrick, Frederick, MD 21702-5012			10. SPONSORING/MONITORING AGENCY REPORT NUMBER	
11. SUPPLEMENTARY NOTES <div style="text-align: right; font-size: 2em; font-weight: bold;">19990528 043</div>				
12a. DISTRIBUTION / AVAILABILITY STATEMENT Approved for public release; distribution unlimited			12b. DISTRIBUTION CODE	
13. ABSTRACT (Maximum 200) Ceramide has emerged as an important intracellular regulator of cell growth and viability. In breast carcinoma cells, we find that tumor necrosis factor α (TNF α) causes prolonged and significant accumulation of ceramide, which precedes cell death. We have investigated the mechanism of ceramide formation and the mechanism of ceramide action. This accumulation of ceramide involves activation of ICE-like proteases which are inhibitable by CrmA. On the other hand, the addition of ceramide to cells results in the induction of apoptosis which is inhibited by Bcl-2 and by inhibitors of the caspase-3-type proteases (DEVD). In further examination of the mechanism of ceramide formation, we have determined that TNF α causes activation of neutral sphingomyelinase through a drop in glutathione levels. The addition of GSH to TNF α -treated cells results in replenishment of glutathione levels, prevention of ceramide formation, and partial inhibition of cell death. In additional studies, we find that ceramide activates protein phosphatases which appear to mediate the effects of ceramide on growth. These studies are beginning to elucidate the mechanisms involved in activation of sphingomyelinase by TNF α and the role of ceramide in mediating apoptosis and cell cycle arrest in breast carcinoma cells.				
14. SUBJECT TERMS Ceramide, Lipid Second Messengers, Sphingolipids, Apoptosis, Cell Growth Regulation, Signal Transduction, Retinoblastoma, Protein Kinases, Breast Cancer			15. NUMBER OF PAGES 40	
			16. PRICE CODE	
17. SECURITY CLASSIFICATION OF REPORT Unclassified	18. SECURITY CLASSIFICATION OF THIS PAGE Unclassified	19. SECURITY CLASSIFICATION OF ABSTRACT Unclassified	20. LIMITATION OF ABSTRACT Unlimited	

FOREWORD

Opinions, interpretations, conclusions and recommendations are those of the author and are not necessarily endorsed by the U.S. Army.

____ Where copyrighted material is quoted, permission has been obtained to use such material.

____ Where material from documents designated for limited distribution is quoted, permission has been obtained to use the material.

XH Citations of commercial organizations and trade names in this report do not constitute an official Department of Army endorsement or approval of the products or services of these organizations.

____ In conducting research using animals, the investigator(s) adhered to the "Guide for the Care and Use of Laboratory Animals," prepared by the Committee on Care and use of Laboratory Animals of the Institute of Laboratory Resources, national Research Council (NIH Publication No. 86-23, Revised 1985).

____ For the protection of human subjects, the investigator(s) adhered to policies of applicable Federal Law 45 CFR 46.

YH In conducting research utilizing recombinant DNA technology, the investigator(s) adhered to current guidelines promulgated by the National Institutes of Health.

YH In the conduct of research utilizing recombinant DNA, the investigator(s) adhered to the NIH Guidelines for Research Involving Recombinant DNA Molecules.

YH In the conduct of research involving hazardous organisms, the investigator(s) adhered to the CDC-NIH Guide for Biosafety in Microbiological and Biomedical Laboratories.

C. J. [Signature]
PI - Signature

10/2/98
Date

TABLE OF CONTENTS

1. Front Cover
2. Report Documentation Page
3. Foreword
4. Table of Contents
5. Introduction
- 6-11. Body
12. Conclusions
- 13-14. References
- 15-39. Appendix: Figures
40. Bibliography and list of personnel

INTRODUCTION

Ceramide has recently emerged as an important endogenous candidate mediator of growth suppression; especially in response to cytotoxic agents and stress stimuli (1-3). Briefly, a number of extracellular agents have been found to induce ceramide formation. These include: Tumor Necrosis Factor alpha (TNF α), γ interferon, interleukin-1 β , dexamethasone, Fas ligands, chemotherapeutic agents, and nerve growth factor (4). These agents cause the activation of membrane sphingomyelinases, which act on membrane sphingomyelin, causing the formation of ceramide. The addition of analogs of ceramide to cells causes either terminal cell differentiation, cell senescence, cell cycle arrest, or apoptosis. A role for the endogenous ceramide in mediating these biological effects in response to the above listed agents is further supported by the close association of formation of endogenous ceramide with these biological outcomes, the ability of exogenous ceramides to mimic these biologies, and the ability of agents that interfere with ceramide metabolism to modulate these responses (5,6).

The role of ceramide is further supported by recent insight into the mechanism of action of ceramide *in vitro* and in cells. Thus, *in vitro* ceramide has been shown to activate a serine/threonine protein phosphatase (7). This phosphatase is inhibited by okadaic acid, and okadaic acid appears to inhibit the effects of ceramide on apoptosis and growth suppression (8). Furthermore, an equivalent pathway has been demonstrated in yeast cells, whereby ceramide causes growth suppression of yeast (9). Genetic evidence was provided for the subunit composition of this phosphatase in yeast (10). Deletion of these subunits in yeast results in resistance to the activity of ceramide on growth suppression. Taken together, these studies suggest that ceramide in yeast works through activation of this phosphatase. Coupled with the inhibitor studies in mammalian cells, these studies would also suggest a role for this phosphatase in mediating the effect of ceramide on growth suppression.

In addition, ceramide has been shown to modulate a number of biochemical events in cells. For example, ceramide has been shown to activate the retinoblastoma gene product, down regulate the c-myc oncogene, inhibit phospholipase-D, modulate protein phosphorylation, activate protein kinases, and inhibit protein kinase C α (8,11-14).

Major questions in this area of research center on: (1) What are the mechanisms involved in ceramide formation? (2) What are the mechanisms by which ceramide causes growth suppression? and (3) What is the precise role of ceramide in mediating growth suppression in response to TNF α , chemotherapeutic agents, and the other extracellular agents and stimuli that cause ceramide formation? The results accumulated during the conduct of this proposal have provided significant insight aimed at addressing these issues. In particular, we have shown that TNF α causes accumulation of ceramide which precedes cell death, and it induces activation of at least two distinct classes of proteases. The first class is involved in induction of ceramide levels and these are inhibited by CrmA and by YVAD. The second class is activated by ceramide and seems to act downstream to ceramide accumulation. Activation of these proteases is inhibited by Bcl-2 and by DEVD. In further studies, we demonstrate that there is a direct and mechanistic relationship between oxidative stress signaling and ceramide accumulation. We find that TNF α causes a drop in glutathione (GSH) levels and that this drop results directly in activation of neutral sphingomyelinase and accumulation of ceramide. These studies define for the first time a fundamental biochemical mechanism for coupling of the cytokine action to oxidative stress to ceramide formation and ceramide-mediated biology. In additional studies, we find that ceramide activates the protein phosphatase PP1 which appears responsible for mediating the growth effects of ceramide. These results should be of significance in defining mechanisms of tumor cell death.

BODY

Experimental Methods:

Tissue culture. Cells were grown in RPMI 1640 medium supplemented with 10% fetal bovine serum (FBS) and 0.2% sodium bicarbonate. G418 at 500 $\mu\text{g/ml}$ was added to the CrmA cell line and its vector while hygromycin 150 $\mu\text{g/ml}$ was added to the Bcl-2 cell line and its vector. Experiments were done in the absence of G418 or hygromycin. Cell viability was determined by the ability to exclude trypan blue.

Partial Purification of N-SMase -MCF7 cells grown to near confluence in 175 cm^2 flasks were harvested by trypsinization, washed with ice-cold phosphate buffered saline (PBS), pelleted by centrifugation, frozen in a methanol-dry ice bath and stored at -80°C until use. To obtain N-SMase, detergent solubilized membrane proteins were prepared from homogenate from pooled cell pellets (2×10^9 cells) and resolved on a DEAE-Sepharose column ($1 \times 10 \text{ cm}$) connected to a Pharmacia FPLC system essentially as described (16), except that both buffers A and B contained Triton X-100 (0.005%, w/v). N-SMase was efficiently resolved from A-SMase in MCF7 cells (17) by the detergent extraction step and DEAE column, such that the final N-SMase preparation contained $<1\%$ of A-SMase activity under the assay conditions.

N-SMase Activity Assay--The activity of N-SMase was determined using a mixed micelle assay system as described (16). The reaction mixture contained enzyme preparation in 100 mM Tris-HCl, pH 7.4, 10 nmol [^{14}C]sphingomyelin (100,000 DPM), 0.1% Triton X-100 and 5 mM magnesium chloride in a final volume of 100 μl .

Measurement of Ceramide--Cells grown in 10 cm petri dishes were rinsed with ice-cold PBS and scraped into methanol. Cell lipids were extracted by the method of Bligh and Dyer (15). Ceramide content was determined using a modified diacylglycerol kinase assay as previously described (18).

SM level-- Cells were seeded at 2×10^5 cells/10 cm culture dish and grown for 48 hr. Then cells were switched to fresh complete medium containing [^3H]choline (1 $\mu\text{Ci/ml}$). After 48 hrs, cells were switched again to fresh medium and chased for 2 hr before treatment with GSH and/or TNFa as described above. The level of SM was determined following a protocol essentially as described (19).

Measurement of GSH Level - Cells were seeded at 2×10^5 in 6 cm petri dishes in 4 ml of complete medium. Two days later, cells were treated with the desired agents as described above. Treated cells were detached by trypsinization, washed (3X) with ice-cold PBS and solubilized in 150 μl of water. 5-sulphosalicylic acid was added to a final concentration of 2% and the supernatant was separated from the acid precipitated proteins by centrifugation. GSH content in the supernatant was determined by the Griffith (20) modification of the Tietze's enzymatic procedure (22) as described (16). Protein content was determined by the dye binding assay using bovine serum albumin as standard (23).

Transfection and expression of Bcl-2. Cells were transfected with either the vector pMEP4 alone or vector containing Bcl-2 using Lipofectamine. Cells were then selected with Hygromycin B1. Expression of Bcl-2 was confirmed by western blot analysis.

Western blot for PARP-Cells were scraped into medium, pelleted by centrifugation, and washed (1X) with ice cold PBS containing 1 mM PMSF. The cell pellet was resuspended in 50 μl of PBS-PMSF and solubilized in 2X SDS sample buffer. Western blot for PARP was performed as described (18,24).

Western Blots for the retinoblastoma gene product (Rb). The status of Rb phosphorylation was determined using Western Blot analysis as described above. The hypophosphorylated Rb migrates faster than the phosphorylated species.

Phosphatase assay for [^{32}P]-Rb in vitro. Cells were labeled with 1 mCi/ml [^{32}P]-orthophosphate in serum-free, phosphate-free DMEM for 3-4 hrs. Cells were lysed with lysis buffer as described elsewhere (Lee et al., manuscript in preparation). The cleared lysates were immunoprecipitated with anti Rb antibody and protein A-sepharose. The immunocomplexes were washed and used for *in vitro* phosphatase assay as the substrate. Dephosphorylation reactions contained 50 mM Tris-HCl, 1 mM EDTA, pH 7.4, PP1 and the indicated amount of radiolabeled substrate in a final volume of 0.1 ml. Ceramide or other lipids were delivered in 1 ml of absolute ethanol to give the indicated concentrations. Control assays received a similar volume of ethanol. Reactions were initiated with the addition of substrate and incubated for 15 min at 30 °C. Assays were terminated with 0.1 ml of 1 mM KH_2PO_4 in 1 N H_2SO_4 and 0.3 ml of 2% ammonium molybdate. After standing for at least 10 min, free ^{32}P i was determined as organic extractable counts after the addition of toluene:isobutyl alcohol(1:1). The amount of organic extractable ^{32}P i in blank assay was typically <0.1% of total radioactivity added. [^{32}P]-MBP hydrolysis was linear with respect to time and protein and did not exceed 15% of total MBP added.

Cell viability-The viability of cells was determined by their ability to exclude trypan blue. The survival of cells was determined with the WST-1 cell proliferation reagent from Boehringer Mannheim. Cells were seeded at 10^3 cells/well/200 μl of complete medium in 96-well culture plate. Two days later, cells were treated in quadruplicate with $\text{TNF}\alpha$ as described above. At the end of treatment, WST-1 reagent was added and after a 3 hr incubation period, the absorbance was measured at 450 nm with a multi-well plate reader as recommended by the manufacturer.

RESULTS:

$\text{TNF}\alpha$ causes apoptotic cell death in MCF-7 cells as well as ceramide accumulation, which precedes cell death. MCF-7 breast carcinoma cells were treated with $\text{TNF}\alpha$, and ceramide levels and cell death were evaluated concomitantly at several time-points (Fig. 1). Ceramide levels did not change appreciably in the first 5 hours but were significantly increased between 7 and 9 hours and continued to increase with time; such that the levels of ceramide increased up to 400% by 20 hours. Cell death, as measured by the inability to exclude trypan blue, was not seen until 20 hours; occurring several hours following the increase in ceramide levels, indicating that ceramide accumulation occurs long before loss of membrane integrity.

In order to verify that cell death was occurring through induction of apoptosis, we assayed for cleavage of the 116 kDa poly(ADP-ribose) polymerase (PARP) polypeptide to a specific 85 kDa apoptotic fragment. This proteolytic cleavage has been shown to occur in apoptosis and to be mediated by Yama/CPP32/apopain or related proteases. It is now considered a hallmark of many apoptotic pathways, and it is a reliable parameter to distinguish apoptosis from necrosis. Treatment of MCF-7 cells with $\text{TNF}\alpha$ resulted in specific cleavage of PARP to the 85 kDa fragment (Fig. 2). Significant PARP cleavage did not occur until 12 hours after treatment with $\text{TNF}\alpha$ and was maximal by 25 hours. These results indicate that ceramide accumulation precedes by at least 3-4 hours one of the early signs of apoptosis, i.e. PARP cleavage.

2. *TNF causes cell cycle arrest and activates Rb.* When cells were treated with TNF, we observed a cell cycle phenotype such that treated cells were arrested in the G0/G1 phase of the cell cycle. Treatment with TNF also caused dephosphorylation of Rb in a time dependent manner (Fig. 3). This was of great interest to us since: 1. dephosphorylated Rb appears to be the active species that induces a G0/G1 arrest; and 2. we have previously shown that ceramide causes an Rb-dependent arrest in G0/G1 in Molt-4 cells. Thus, it is tempting to speculate that TNF causes a cell cycle arrest in a ceramide-dependent manner. Current studies aim at examining the effects of ceramide on Rb in MCF-7 cells.

3. *Involvement of proteases in ceramide formation.* The cowpox viral protein, CrmA, is a protease inhibitor which is known to inhibit, with variable efficiency, the ICE family of cysteine proteases. CrmA was utilized in our experiments to examine the relationship of these proteases to ceramide along the death pathway. MCF-7 cells stably expressing CrmA were treated with 2 nM TNF α or increasing concentrations of C₆-ceramide, a cell-permeable ceramide analog, and compared with control (vector) cells. CrmA offered almost complete protection from TNF α -induced cytotoxicity (Fig. 4). However, CrmA offered no protection from the cytotoxic effects of ceramide whereby cells died equally in the presence or absence of CrmA (Fig. 4). Therefore, CrmA appeared not to interfere with the downstream effects of ceramide.

Since endogenous ceramide elevation may drive the cell to die, we next examined whether CrmA interferes with ceramide generation. Endogenous ceramide levels were measured in response to TNF α in control and in CrmA-expressing MCF-7 cells. Ceramide increased significantly in vector cells at 18 and 24 hours (Fig. 5). However, CrmA-expressing cells treated similarly with TNF α showed no increase in ceramide levels. The results with CrmA suggest that proteases are involved in ceramide generation.

4. *Support that bcl-2 acts at the point downstream of ceramide but upstream of activation of the death proteases.* Since ceramide generation occurred in cells that eventually die in response to treatment with TNF α and not in the protected, CrmA-expressing cells, it became important to verify that this increase in ceramide levels, as well as the suppression of this increase by CrmA, were not nonspecific events correlating with cell death or survival, respectively. We utilized Bcl-2, another antiapoptotic molecule. MCF-7 cells expressing Bcl-2 or vector controls were treated with TNF α or increasing concentrations of C₆-ceramide. Control cells died in response to both treatments but Bcl-2-expressing cells displayed resistance to TNF α -induced cell death as seen in cells expressing CrmA (Fig. 6). However, unlike CrmA-expressing cells, Bcl-2-expressing cells were resistant to ceramide-induced cell death. Additionally, generation of endogenous ceramide was nearly equal in both vector and Bcl-2 cells in response to TNF α , indicating that Bcl-2 does not interfere with ceramide generation (Fig. 7). Therefore, Bcl-2 functions at a point downstream of ceramide to inhibit apoptosis. More importantly, this delayed accumulation of ceramide is not a consequence of cell death since it is still observed in the viable Bcl-2 expressing cells. Thus, these data demonstrate that the elevation in ceramide is proximal to the biochemical and morphological changes of cell death.

5. *GSH Reversibly Inhibits Neutral SMase in vitro*—Previously we found that GSH inhibited *in vitro* the N-SMase from Molt-4 leukemic cells (16). To study the role of GSH in TNF α signaling, we chose the human mammary carcinoma cell line MCF7 which is very sensitive to TNF α . We partially purified N-SMase from MCF7 cells following the procedure described for rat brain (16) and tested the effects of GSH on N-SMase *in vitro*. When, the enzyme was preincubated for 5 min at 37°C with 1-20 mM GSH followed by incubation with substrate for 30 min, a dose-dependent inhibition of N-SMase by GSH was observed with a greater than 95%

inhibition observed with 3 mM of GSH (Fig. 8). The inhibition was specific for GSH since two other small thiol-containing molecules, dithiothreitol (DTT) and b-mercaptoethanol, at concentrations up to 20 mM, were ineffective (Fig 8). These results demonstrate that physiologic levels of GSH (3-10 mM) totally inhibit N-SMase. The results also suggest that the sharp drop in cellular levels of GSH may relieve this inhibition and cause activation of N-SMase.

6. *GSH Reversibly Inhibits Neutral SMase in cells*—To investigate the effect of GSH on N-SMase in TNF α signaling, MCF7 cells were treated with TNF α (3 nM) for 2-24 hr and GSH levels were measured. As shown in Figure 9A, TNF α treatment resulted in an initial sharp drop in the level of GSH followed by a steady further decrease, with the first significant decrease observed at 8 hr post treatment. The most dramatic change in the level of GSH occurred between 8 and 10 hr post TNF α treatment where the GSH level plunged to nearly a third of that of control cells at the 10 hr time point. GSH levels then steadily decreased to 7% of control cells by 24 hr (Fig. 9A). At the 10 hr time point, cells treated with TNF α did not manifest any detectable sign of apoptosis. In particular, proteolysis of the "cell death substrate" poly(ADP-ribose)polymerase (PARP) was only detected at 12-24 hr (17). When the effect of TNF α on cellular SM level was examined, significant SM hydrolysis was observed between 10 and 16 hr, and a 30% hydrolysis of SM was detected at 14 hr (Fig. 9B). These kinetics raise the possibility that GSH may be involved in the regulation of SM hydrolysis and ceramide generation in cells treated with TNF α .

Since GSH inhibited N-SMase *in vitro* at physiologically relevant concentrations and changes of GSH levels induced by TNF α proceeded ceramide accumulation and SM hydrolysis, we next investigated the effects of manipulating intracellular GSH levels on TNF α -induced SM hydrolysis and ceramide generation. First, replenishment of intracellular GSH by addition of 10 mM GSH to the culture medium prior to TNF α treatment (3 nM; 14 hr) completely prevented the TNF α -induced SM hydrolysis (Fig. 10A). Treatment of cells with GSH (10 mM) alone had no effect on SM levels. Second, GSH pretreatment significantly inhibited the accumulation of ceramide induced by TNF α (Fig. 10B). A nearly complete inhibition of ceramide increase was observed at 12 hr post TNF α treatment (Fig. 10B). At 16 and 24 hr, ceramide accumulation induced by TNF α was inhibited by about 50%. Third, in addition to GSH, significant inhibition of TNF α -induced ceramide accumulation was also achieved by treatment of cells with GSH methylester and N-acetylcysteine (NAC) which is converted intracellularly to cysteine, a precursor of GSH biosynthesis (Fig. 10C). These results further support the notion that GSH levels regulate the activity of N-SMase in these cells.

7. *Involvement of GSH in TNF-induced cell death*—Next, the biological consequences of changes in GSH levels in response to TNF α were studied by examination of cell death and survival. Whereas TNF α induced significant cell death, as determined by the ability of cells to exclude trypan blue dye, partial rescue of cells was achieved by replenishment of intracellular GSH with GSH added to the cell culture medium. Preincubation of cells with 10 and 15 mM GSH for 2 hr prior to treatment with TNF α lowered TNF α -induced cell death from 58.5% to 35.5% and 26.5% respectively (Fig. 11A). The effect of TNF α on the viability of MCF7 cells was also determined using the WST-1 assay which measures the activity of the mitochondrial respiratory chain in viable cells. TNF α significantly reduced the survival of MCF7 cells, and a 50% reduction in survival was observed when cells were treated with 1 nM TNF α for 24 hr (Fig. 11B). Inclusion of 10 mM GSH enhanced the survival of TNF α -treated cells to 75-95% of control level (Fig. 11B).

Mechanistically, the effects of TNF α on PARP cleavage, a close marker of the apoptotic response, were evaluated. TNF α -induced cleavage of PARP was partially inhibited by GSH and NAC in a dose-dependent manner (Fig. 11C). Since PARP is a substrate for "execution" phase proteases such as CPP32/caspase-3, these results place GSH upstream of these proteases in the pathways leading to cell death.

8. *Relationship of GSH levels to caspase activation and to Bcl-2 - TNF α -induced accumulation of ceramide* has been shown to be inhibited by the cow pox virus cytokine modifier protein (crmA) but not by bcl-2 (see above), placing activation of SMases downstream of crmA-inhibitable proteases and upstream of bcl-2 inhibitable proteases. To investigate the relationship between crmA and GSH, MCF7 transfected with crmA or empty vector were treated with TNF α , and GSH levels were determined. No significant changes in GSH levels were observed in crmA-transfected cells treated with 3 nM TNF α over a time period ranging from 1 to 24 hr whereas a time dependent depletion of GSH was observed in the vector-transfected cells (Fig. 12A). The TNF α -induced depletion of GSH was also inhibited in a dose dependent manner by the substrate-based tetrapeptide inhibitor of ICE proteases, YVAD-chloromethylketone. Pretreatment of MCF7 cells with 50 μ M YVAD prior to TNF α (3 nM) brought the GSH level from 20% of control to 80% of control (Fig. 12B). These results clearly demonstrate that the drop in GSH in response to TNF α is dependent upon activation of ICE-like proteases (such as caspases-8/FLICE).

9. *Effects of ceramides on PP1 activity for [32 P]-MBP in vitro* In order to examine a possible effect of ceramide on PP1, the recombinant catalytic subunit of PP1a (rabbit muscle) was incubated in the presence of increasing concentrations of C₆-ceramide. The catalytic subunit of PP1a was stimulated by C₆-ceramide in a dose-dependent manner. When assayed with 5-150 μ g/ml 32 P-MBP, maximal stimulation occurred at 30 μ M C₆-ceramide, with 2-3 fold stimulation over baseline (Fig. 13).

10. *Specificity of ceramide activation of PP1* Previous work from our laboratory indicated that dihydroceramide lacks the bioactivity profile characteristic of ceramide in causing Rb dephosphorylation, cell cycle arrest or apoptosis. Therefore, the effects of C₂- and C₆-ceramide were compared to those of C₂- and C₆-dihydroceramide. The stimulation of PP1 was specific to the biologically active C₂- and C₆-ceramide as the inactive forms, C₂ and C₆-dihydroceramide (Fig. 14), failed to activate PP1.

11. *Effects of various protein phosphatase inhibitors on Rb dephosphorylation induced by C₆-ceramide in cells*. To identify which phosphatase is involved in the induction of the dephosphorylation of Rb induced by ceramide, we performed the following studies in cells. We examined the effects of okadaic acid or calyculin A on Rb dephosphorylation. Calyculin A (Fig. 15A), but not okadaic acid (Fig. 15B) prevented Rb dephosphorylation induced by C₆-ceramide in a dose-dependent manner. Similarly, calyculin potently inhibited the effects of ceramide on PARP proteolysis (data not shown).

12. *Effects of C₆-ceramide on PP1-induced [32 P]-Rb dephosphorylation in vitro*. Since the above results implicated PP1-like activity in mediating Rb dephosphorylation in cells, we next evaluated for direct *in vitro* effects of C₆-ceramide on PP1-induced Rb dephosphorylation. [32 P]-Rb, immunoprecipitated from cells as described in "Experimental Methods", was dephosphorylated *in vitro* by PP1a. C₆-ceramide, but not C₆-dihydroceramide, activated PP1a-induced Rb dephosphorylation *in vitro* (Fig. 16). These data show that Rb is a direct substrate for PP1, and that ceramide stimulates this dephosphorylation.

Relationship to Goals (from revised statement of work).

Task 1: To determine the mechanism by which TNF and chemotherapeutic agents cause activation of the sphingolipid pathway and cause accumulation of ceramide in breast cancer cells.

We have made substantial progress in defining the mechanisms of accumulation of ceramide, especially in response to TNF α in breast cancer MCF-7 cells. Specifically, we found previously that TNF α causes activation of neutral sphingomyelinase and consequent accumulation of ceramide. This is a delayed response that requires activation of ICE-like proteases which are inhibitable by CrmA and by YVAD. We have made a fundamental observation on a direct mechanism coupling TNF action to activation of neutral sphingomyelinase. From *in vitro* studies, we find that GSH results in inhibition of neutral sphingomyelinase. A drop in GSH levels would therefore result in activation of neutral sphingomyelinase *in vitro* and in cells. This was evaluated with TNF α which was shown in this study to cause a drop in cellular levels of GSH that are mechanistically related to activation of neutral sphingomyelinase.

Task 2: Define the role of ceramide in the regulation of breast cancer cells. In our studies we have shown that ceramide causes activation of proteases of the caspase-3 sub-family of death proteases. This activation is inhibited by bcl-2 and by tetrapeptide inhibitors such as DEVD. Taken together, these studies show that the ability of ceramide to induce apoptosis in MCF-7 cells occurs upstream of the site of action of bcl-2 and involves activation of cell death proteases. These conclusions are further supported by results from this study. The action of GSH on neutral SMase support a role for ceramide, formed through this pathway, in the regulation of proteases and cell death. These results open the way for devising novel approaches at treatment of breast cancer using regulator of ceramide metabolism since these would cause accumulation of ceramide with the result of growth inhibition and apoptosis.

Task 3 Determine the mechanism of action of ceramide and of agents that induce ceramide formation. We have made significant progress in this line of study. We have found (previously) that ceramide activates directly the PP2A protein phosphatase. In recent studies, we find that ceramide also activates PP1 protein phosphatase, and this phosphatase appears to mediate the effects of ceramide on the dephosphorylation (activation) of Rb and to also mediate effects on PARP proteolysis and apoptosis. Taken together, we have now a very advanced blueprint of a possible molecular mechanism for the action of ceramide.

CONCLUSIONS

Studies in the first phase (years 1 and 2) of the proposal demonstrated that operation of the sphingomyelinase-ceramide pathway in MCF-7 cells which is activated by temoxiphen and TNF α . Since the effects of TNF α were early and more robust, we concentrated primarily on this agent to activate the apoptotic pathways in MCF-7 cells. We also documented the ability of TNF α and ceramide to cause apoptosis in this cell line, and studies were initiated evaluating the effects of ceramide and TNF α on cell cycle arrest in this cell line.

During the second phase (years 2 and 3) of the proposal, we made major connections involving TNF α , ceramide, and major known regulators of apoptotic responses. In particular, we showed that TNF α causes the activation of at least two distinct classes of proteases. The first class of proteases which are inhibited by CrmA and by YVAD, and therefore belong to the ICE-like proteases, is activated in response to TNF α and is required for activation of neutral sphingomyelinase and accumulation of ceramide. The second class of proteases which is inhibited by BEVD is probably comprised of caspase-3-type cell death proteases. These proteases are activated by ceramide and by TNF α . The action of TNF α and of ceramide on these proteases is inhibited by DEVD and is inhibited by Bcl-2. Taken together, these studies suggested a sequence of events whereby TNF α causes activation of proximal proteases that result in accumulation of ceramide which then acts through a Bcl-2 inhibitable mechanism to activate downstream cell death proteases.

In the third phase of research (years 3 and 4), we have taken the studies to a more biochemical level and applied those results to a cellular biochemical level. Specifically, we found that GSH plays a critical role in coupling the action of TNF α with activation of the sphingomyelinase-ceramide pathway. These results show that TNF α causes a drop in the cellular levels of glutathione. Because our *in vitro* studies show that glutathione inhibits neutral sphingomyelinase and physiologically relevant concentrations of GSH, these studies suggested to us that this drop in cellular levels of GSH may relieve inhibition of neutral sphingomyelinase and cause activation of this enzyme and subsequent accumulation of ceramide. This was further substantiated by examining the effects of replenishing glutathione following TNF action. This results in inhibition of activation of sphingomyelinase and a drop in ceramide levels. In another mechanistic approach, we have shown that ceramide activates the protein phosphatase PP1 which appears to mediate the effects of ceramide on Rb and on apoptosis.

Taken together, these studies are providing important mechanistic insight both at an *in vitro* biochemical level and at a cellular level into how the apoptotic pathway operates in breast cancer cells, especially in response to TNF α as a primary activator of cell death in these cells. Our studies show for the first time a direct correlation and mechanistic interaction between oxidative stress (which results in a drop in GSH levels) and the ceramide pathway of apoptosis regulation. Our studies also show for the first time how protein phosphatase may play a critical role in coupling sphingolipid metabolism (ceramide accumulation) to the regulation of protein phosphorylation/dephosphorylation.

REFERENCES

1. Hannun, Y. A., L. M. Obeid, and R. A. Wolff. 1993. The novel second messenger ceramide: Identification, mechanism of action, and cellular activity. *Adv. Lipid Res.* 25:43-62.
2. Hannun, Y. A. and L. M. Obeid. 1995. Ceramide: An intracellular signal for apoptosis. *Trends Biochem. Sci.* 20:73-77.
3. Zhang, Y. H. and R. Kolesnick. 1995. Signaling through the sphingomyelin pathway. *Endocrinology* 136:4157-4160.
4. Hanafin, N. M., K. S. Persons, and M. F. Holick. 1995. Increased PKC activity in cultured human keratinocytes and fibroblasts after treatment with 1 α ,25-dihydroxyvitamin D₃. *J. Cell. Biochem.* 57:362-370.
5. Pushkareva, M., L. M. Obeid, and Y. A. Hannun. 1995. Ceramide: An endogenous regulator of apoptosis and growth suppression. *Immunol. Today* 16:294-297.
6. Hannun, Y. A. 1994. The Sphingomyelin cycle and the second messenger function of ceramide. *J. Biol. Chem.* 269:3125-3128.
7. Dobrowsky, R. T. and Y. A. Hannun. 1993. Ceramide-activated protein phosphatase: Partial purification and relationship to protein phosphatase 2A. *Adv. Lipid Res.* 25:91-104.
8. Wolff, R. A., R. T. Dobrowsky, A. Bielawska, L. M. Obeid, and Y. A. Hannun. 1994. Role of ceramide-activated protein phosphatase in ceramide-mediated signal transduction. *J. Biol. Chem.* 269:19605-19609.
9. Fishbein, J. D., R. T. Dobrowsky, A. Bielawska, S. Garrett, and Y. A. Hannun. 1993. Ceramide-mediated biology and CAPP are conserved in *Saccharomyces cerevisiae*. *J. Biol. Chem.* 268:9255-9261.
10. Nickels, J. T. and J. R. Broach. 1996. A ceramide-activated protein phosphatase mediates ceramide-induced G₁ arrest of *Saccharomyces cerevisiae*. *Genes Dev.* 10:382-394.
11. Dbaiibo, G., M. Y. Pushkareva, S. Jayadev, J. K. Schwartz, J. M. Horowitz, L. M. Obeid, and Y. A. Hannun. 1995. Rb as a downstream target for a ceramide-dependent pathway of growth arrest. *Proc. Natl. Acad. Sci. USA* 92:1347-1351.
12. Venable, M. E., G. C. Blobe, and L. M. Obeid. 1994. Identification of a defect in the phospholipase D/Diacylglycerol pathway in cellular senescence. *J. Biol. Chem.* 269:26040-26044.
13. Lee, J. Y., Y. A. Hannun, and L. M. Obeid. 1996. Ceramide inactivates cellular protein kinase Ca. *J. Biol. Chem.* 271:13169-13174.
14. Mathias, S., K. A. Dressler, and R. N. Kolesnick. 1991. Characterization of a ceramide-activated protein kinase: Stimulation by tumor necrosis factor α . *Proc. Natl. Acad. Sci. USA* 88:10009-10013.
15. Bligh, E. G. and W. J. Dyer. 1959. A rapid method of total lipid extraction and purification. *Can. J. Biochem. Phys.* 37:911-917.

16. Liu, B. and Hannun, Y. A. (1997) Inhibition of Neutral magnesium-dependent sphingomyelinase by glutathione. *J. Biol. Chem.* **272**, 16281-16287
17. Liu, B., Obeid, L. M., and Hannun, Y. A. (1997) Sphingomyelinases in cell regulation *Semin. Cell Develop. Biol.* **8**, 311-322
18. Dbaibo, G. S., Perry, D. K., Gamard, C. J., Platt, R., Poirier, G. G., Obeid, L. M., and Hannun, Y. A. (1997) *J Exp. Med.* **185**, 481-490
19. Andrieu, N., Salvayre, R., and Levade, T. (1994) *Biochem. J.* **303**, 341-345
20. Griffith, O. W. (1980) *Anal. Biochem.* **106**, 207-212
21. Tietze, F. (1969) *Anal. Biochem.* **27**, 502-522
22. Bradford, M. M. (1976) *Anal. Biochem.* **72**, 248-254
23. Zhang, P., Liu, B., Jenkins, G. M., Hannun, Y. A., and Obeid, L. M. (1997) Expression of Neutral Sphingomyelinase identifies a distinct pool of sphingomyelin involved in apoptosis. *J. Biol. Chem.* **272**, 9609-9612

APPENDIX

FIGURE LEGENDS

Figure 1. TNF causes cell death and ceramide accumulation in MCF-7 breast carcinoma cells. MCF-7 cells were treated with 2 nM TNF and ceramide and cell death were quantitated as described in methods.

Figure 2. TNF causes apoptosis of MCF-7 cells as determined by proteolysis of PARP. Shown is a time course for PARP proteolysis in cells treated with 2 nM TNF. PARP cleavage was monitored by Western blot analysis as described in the text.

Figure 3. TNF and ceramide cause dephosphorylation of Rb in MCF-7 cells. MCF-7 cells were treated with the indicated concentrations of TNF or ceramide. Proteins were harvested at the indicated time points and Rb phosphorylation/dephosphorylation was evaluated by Western Blotting.

Figure 4. CrmA protects from TNF but not from ceramide induced cell death. MCF-7 cells were treated with the indicated concentrations of ceramide or TNF and cell death was evaluated as described in methods. CrmA-expressing cells were protected from TNF when compared to vector cells.

Figure 5. CrmA inhibits ceramide formation. MCF-7 cells were treated with 2 nM of TNF and ceramide levels were quantitated as described in methods.

Figure 6. Bcl-2 inhibits TNF and ceramide-induced death of MCF-7 cells. Cells overexpressing Bcl-2 were protected from death in response to either TNF or ceramide.

Figure 7. Bcl-2 does not suppress ceramide levels in cells treated with TNF. Cells were treated with 2nM of TNF and lipids were extracted and ceramide was measured as described in methods.

Fig. 8. GSH inhibits N-SMase from MCF7 cells. GSH, but not dithiothreitol (DTT) or b-mercaptoethanol(b-ME), inhibits N-SMase. N-SMase, partially purified from membranes of MCF7 cells, was preincubated for 5 min at 37°C in with the indicated concentrations of GSH, dithiothreitol (DTT) or b-mercaptoethanol (b-ME) followed by the addition of [¹⁴C]-sphingomyelin. Results shown are averages of duplicate determination and are representative of three separate experiments.

Fig. 9. Effect of TNF α on cellular content of GSH and sphingomyelin. A, GSH levels. MCF7 cells were treated with 3 nM TNF α for the indicated time intervals. Total cellular GSH was measured with an enzymatic kinetic assay as described under "Experimental Procedures", normalized against total cellular protein, and expressed as a percentage of the time-matched controls. Results are expressed as percent of time-matched controls and are means \pm S. D. of duplicate determinations of three separate experiments. B, SM levels. MCF7 cells (50% confluent) were pre-labeled with [³H]choline chloride for 48 hr. Cells were treated with 3 nM TNF α for the indicated time intervals. Total cellular lipids were harvested, SM content was determined as described under "Experimental Procedures", and normalized against total cellular protein. Results for B are expressed as percent of time-matched controls and are means \pm S. D. of duplicate determinations of four separate experiments.

Fig. 10. GSH inhibits SM hydrolysis and ceramide accumulation induced by TNF α . A, GSH inhibits TNF α -induced SM hydrolysis. MCF7 cells were pre-labeled with [3H]choline chloride for 48 hr, washed with PBS, and rested for 2 hr in fresh complete medium. Cells were

then pretreated for 2 hr with GSH (10 mM final concentration) before treatment with 3 nM TNF α for 14 hr. SM content was analyzed as described under "Experimental Procedures". Results are expressed as percent of time-matched controls and are means \pm S. D. of duplicate determinations of four separate experiments. * p <0.005 compared to TNF α -treated cells. B, GSH inhibits TNF α -induced ceramide accumulation. MCF7 cells were pretreated with 10 mM GSH for 2 hr followed by 3 nM TNF α for the indicated time intervals. Cellular lipids were extracted and ceramide levels were determined. Results are expressed as percent of time-matched control. * p <0.005 compared to TNF α -treated cells (open circle). C, TNF α -induced ceramide accumulation is inhibited by GSH methylester (GSH-ME) and N-acetylcysteine (NAC). MCF7 cells were pretreated with 10 mM GSH-ME or NAC for 2 hr followed by 3 nM TNF α for 16, or 24 hr. For B and C, ceramide content was determined as described under "Experimental Procedures" and results are expressed as percent of time-matched controls and are means \pm S. D. of duplicate determinations of three separate experiments.

Fig. 11. Elevation of intracellular GSH levels prevents apoptosis induced by TNF α . A, protection of TNF α -induced death by GSH. MCF7 cells were pretreated for 2 hr with 5-15 mM GSH followed by treatment with 3 nM TNF α for 24 hr. Cell death was measured by trypan blue exclusion. Results are means \pm SD of triplicate determinations from three separate experiments. B, GSH inhibits TNF α -induced decrease in cell survival. MCF7 cells cultured in 96-well plate were pretreated for 2 hr with 10 mM GSH followed by treatment with 1-5 nM TNF α for 24 hr. Afterwards, cells were incubated with the WST-1 reagent for 3 hr, and cell survival was analyzed following the manufacturer's instructions. Results are expressed as percent of control and are means \pm SD of quadruplicate determinations from three separate experiments. C, GSH and NAC inhibit TNF α -induced PARP proteolysis. MCF7 cells were pretreated for 2 hr with 10-20 mM GSH followed by treatment with 3 nM TNF α for 18 hr. Cells were scraped into and lysed in SDS sample buffer. The proteins were analyzed with a 6% SDS-PAGE gel and PARP cleavage was analyzed by Western blot as described under "Experimental Procedures". Blot shown is representative of three separate experiments.

Fig. 12. CrmA blocks GSH depletion induced by TNF α . A MCF7 cells overexpressing crmA are resistant to TNF α -induced depletion of GSH. CrmA-, or vector-transfected MCF7 cells were treated with 3 nM TNF α for 2-24 hr. B, YVAD inhibits the TNF α -induced depletion of GSH. MCF7 cells were pretreated for 2 hr with 12.5-50 μ M YVAD followed by treatment with 3 nM TNF α for 12 hr. GSH levels were determined as described under "Experimental Procedures", expressed as percent of time-matched controls, and are means \pm S. D. of duplicate determinations of three experiments.

Fig 13. Activation of recombinant PP1 catalytic subunit by C₆-ceramide. Phosphatase activity of PP1 was assayed by the standard method (0.5-15 mg/ml [³²P]-MBP, for 15 min at 30 °C) using 0 (○), 3 (▲), 10 (■) or 30 μ M (●) C₆-ceramide.

Fig 14 Effect of ceramide and dihydroceramide on PP1. PP1 was assayed as in Fig. 1 in the absence or presence of the indicated concentrations of C₂-ceramide (●) (A) or C₆-ceramide (●) (B) and their dihydro-derivatives (Δ). Phosphatase activity is presented as the activity relative to control in the absence of ceramides. Data are averages \pm S.E. of three separate experiments.

Fig 15. Effect of phosphatase inhibitors on C₆-ceramide-induced Rb dephosphorylation in cells. Rb dephosphorylation was evaluated by Western blot analysis using a monoclonal mouse anti-human antibody in the absence or presence of C₆-ceramide and calyculin A (A), okadaic acid (B). This experiment is representative of three separate experiments.

Fig 16. Effects of C6-ceramide on dephosphorylation of Rb by PP1 *in vitro*. Cells were labeled with [^{32}P]-orthophosphate for 3-4 hrs. Lysates were prepared and [^{32}P]-labeled Rb was immunoprecipitated with anti Rb antibody and protein A-Sepharose. PP1 was assayed as in Fig. 1 using immunoprecipitates as the substrate in the absence or presence of the indicated concentrations of ceramides. Phosphatase activity is presented as the percentage relative to non-specific counts in the absence of PP1. This experiment is representative of two separate experiments.

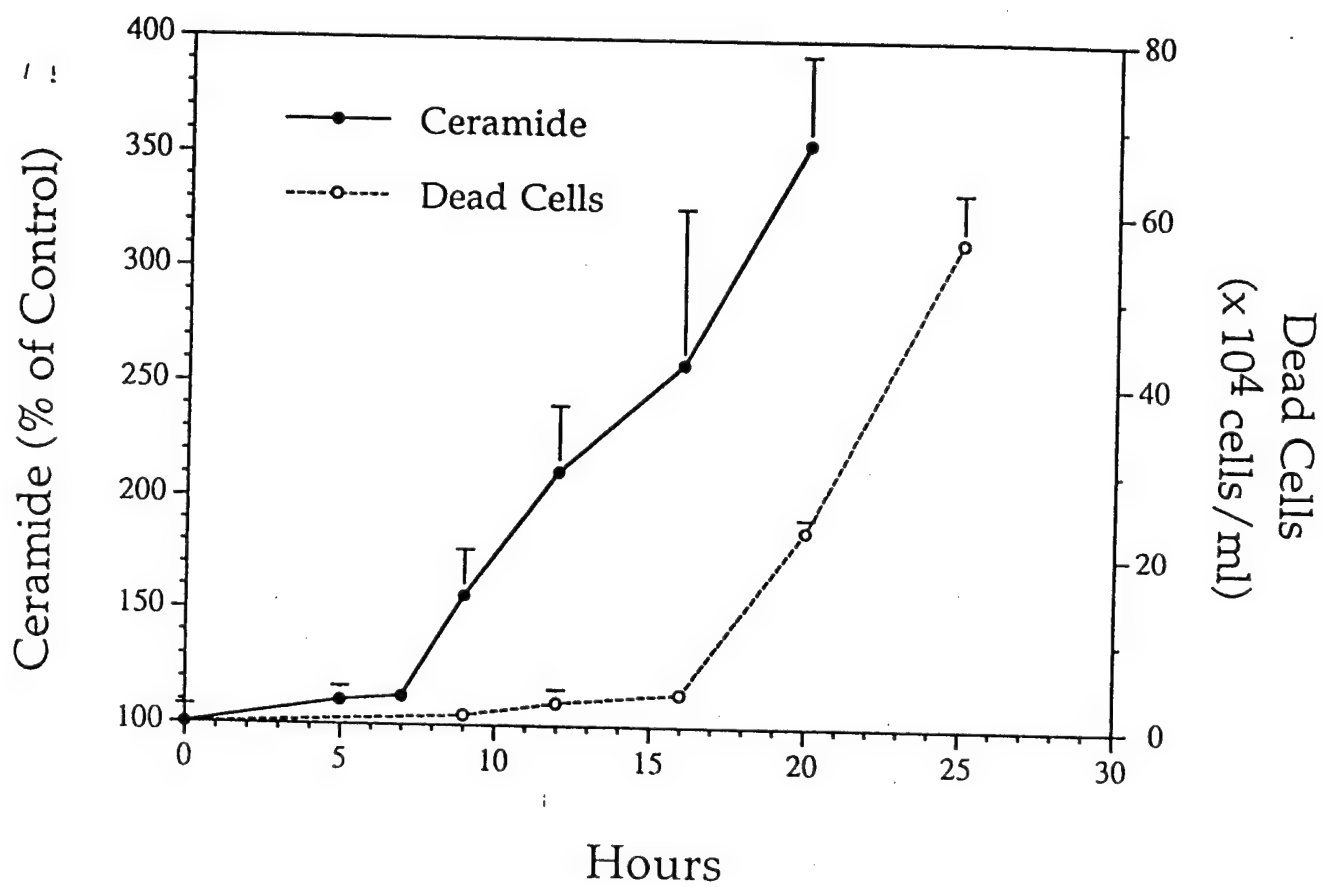


Figure 1

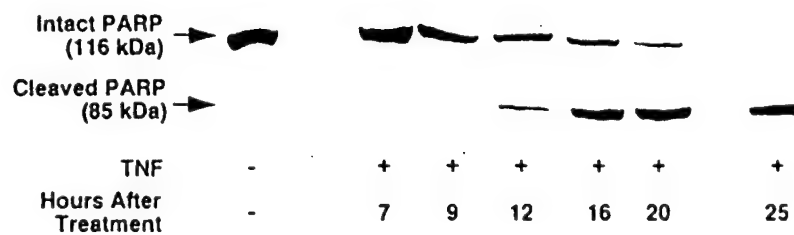
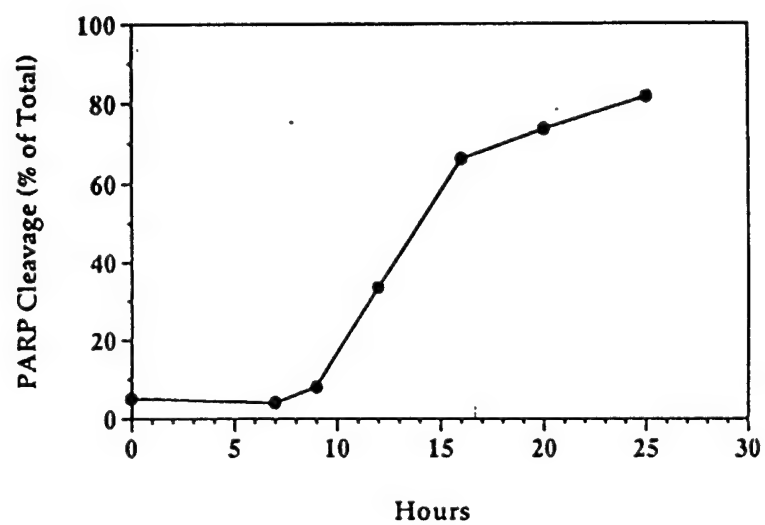


Figure 2

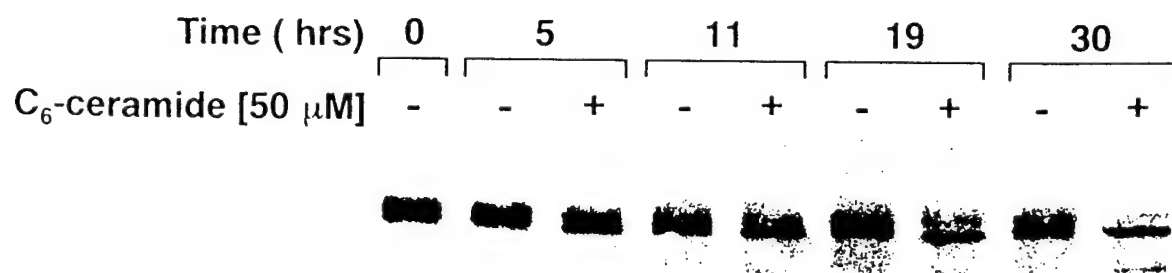
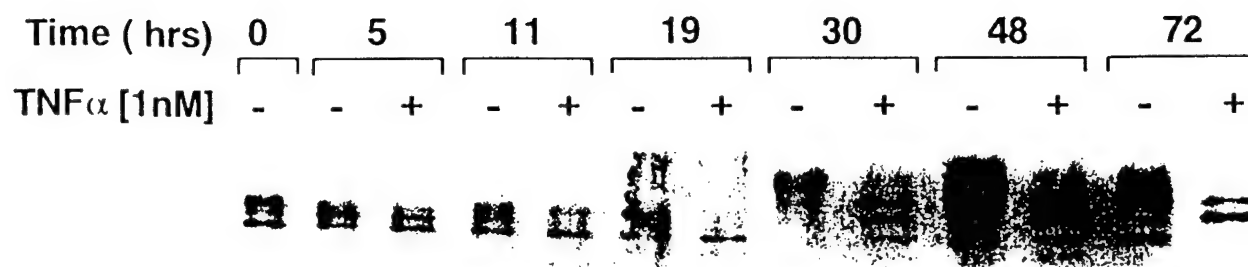


Figure 3

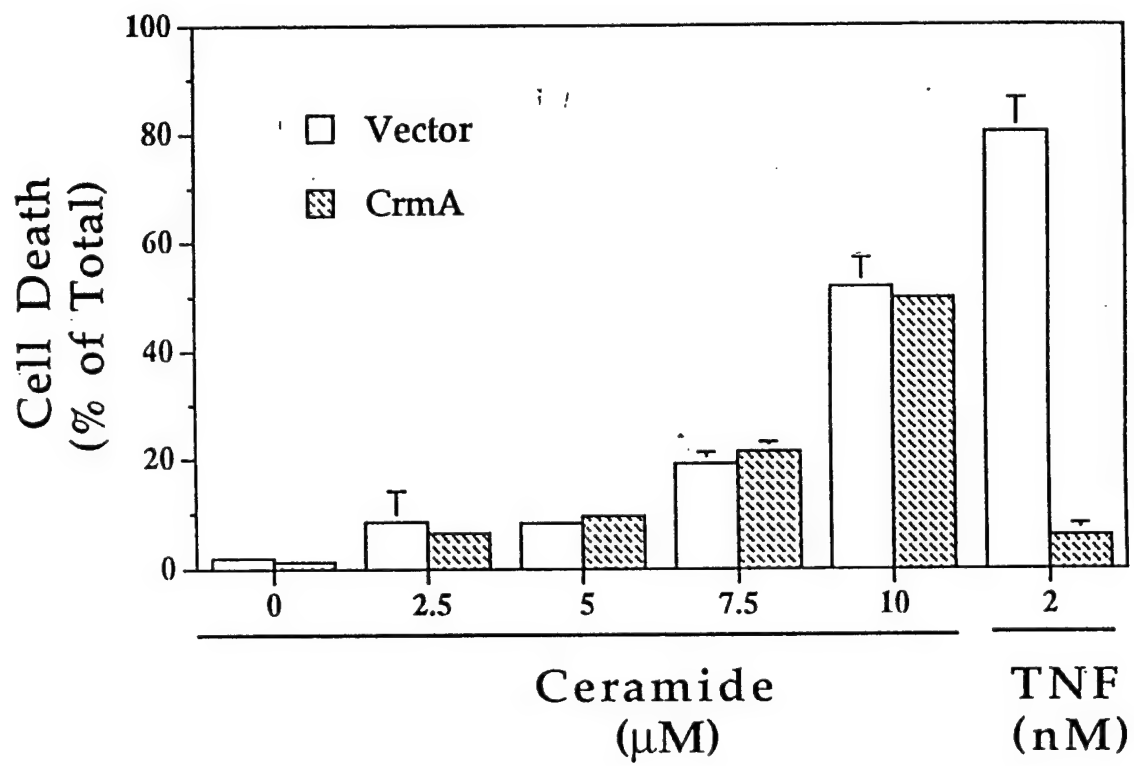


Figure 4

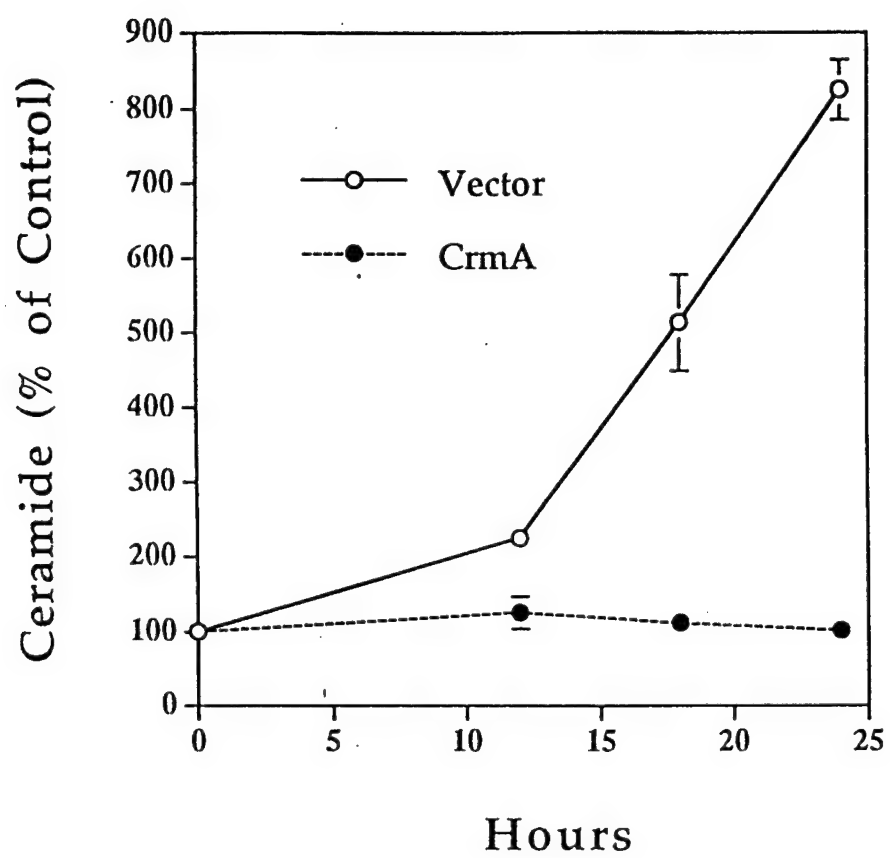


Figure 5

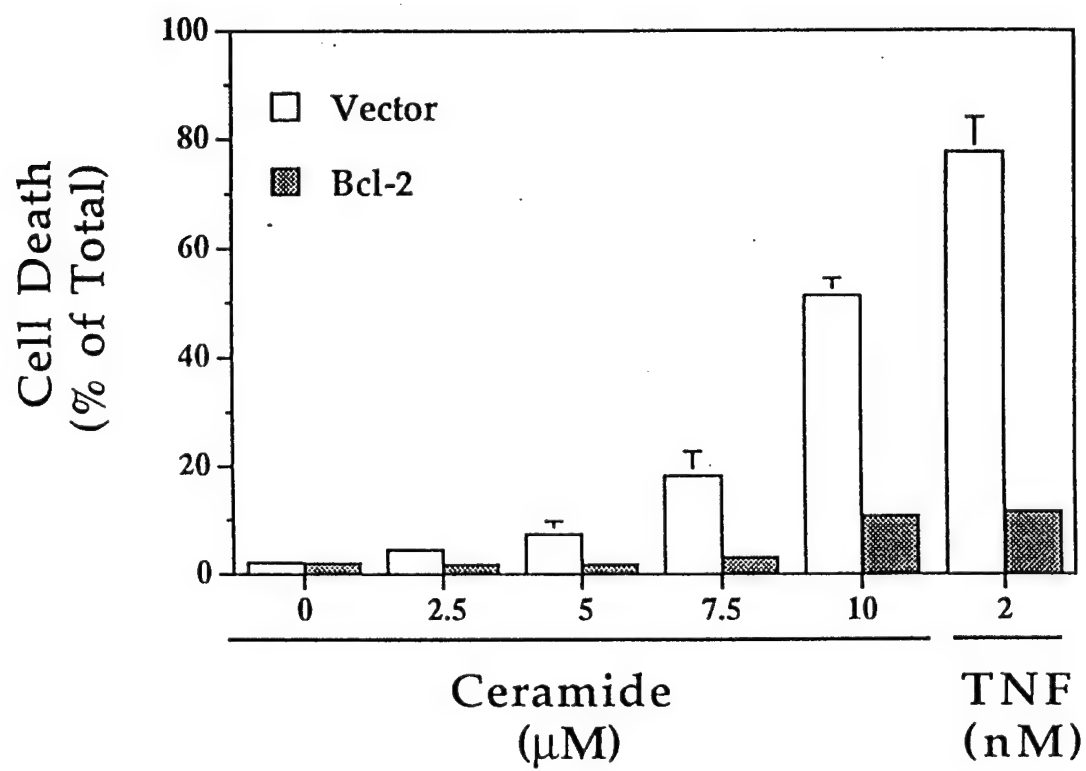


Figure 6

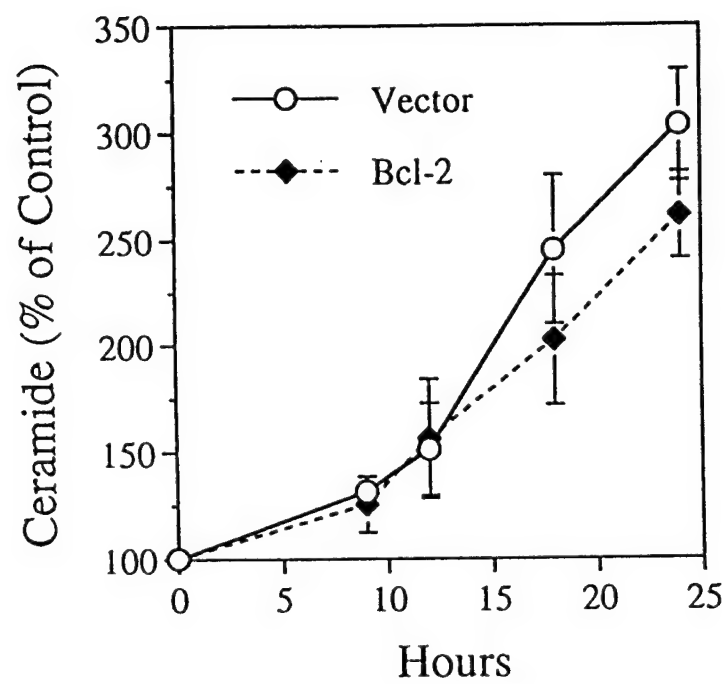


Figure 7

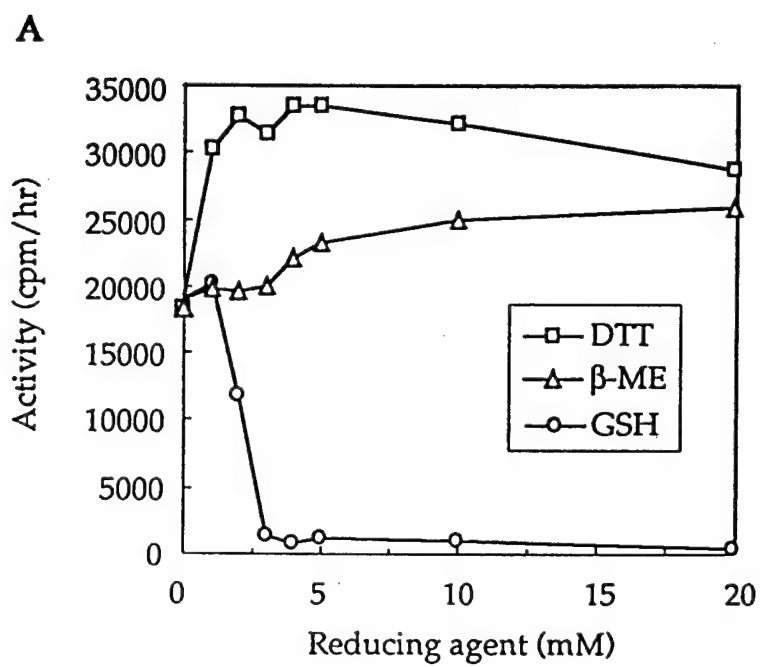


Figure 8

A

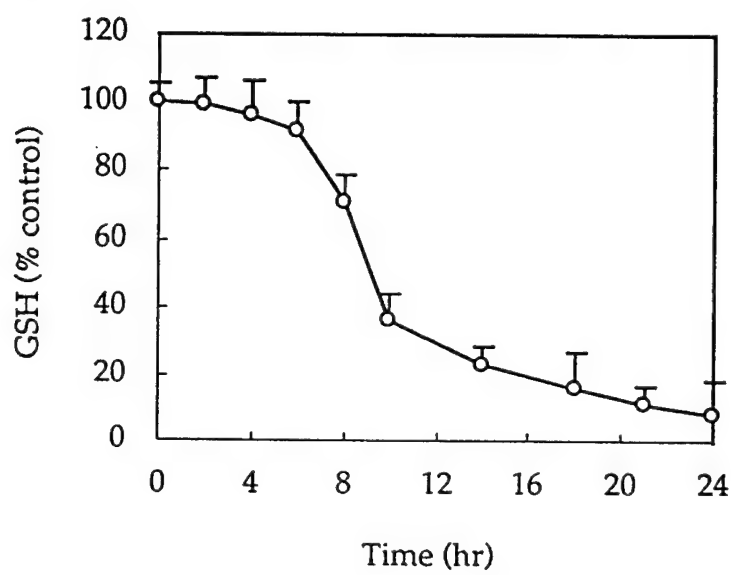


Figure 9A

B

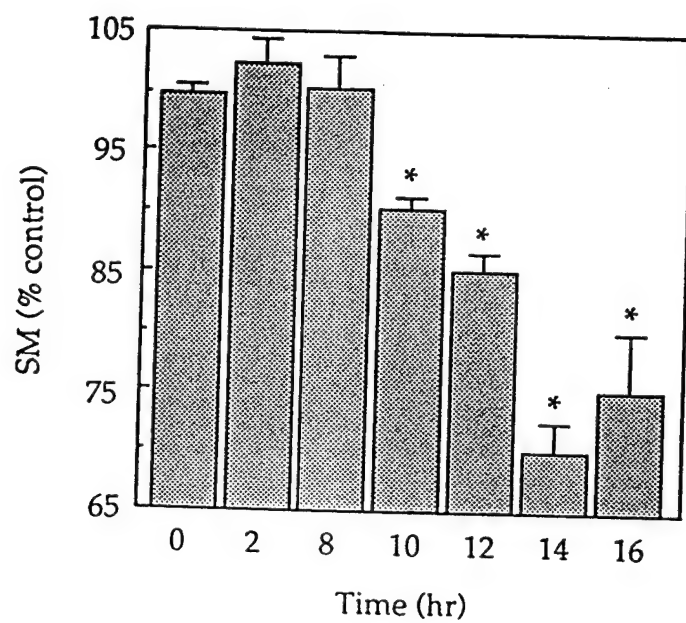


Figure 9B

A

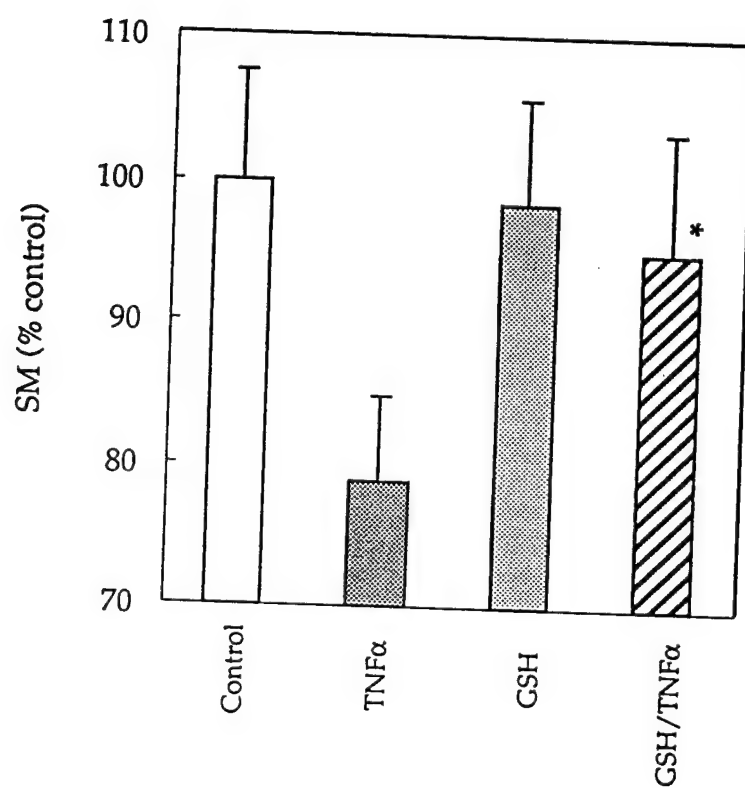


Figure 10A

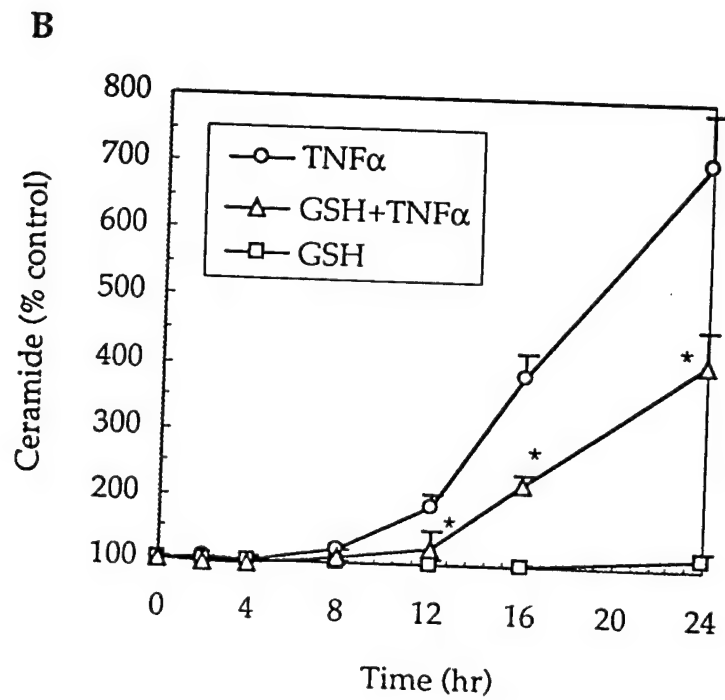


Figure 10B

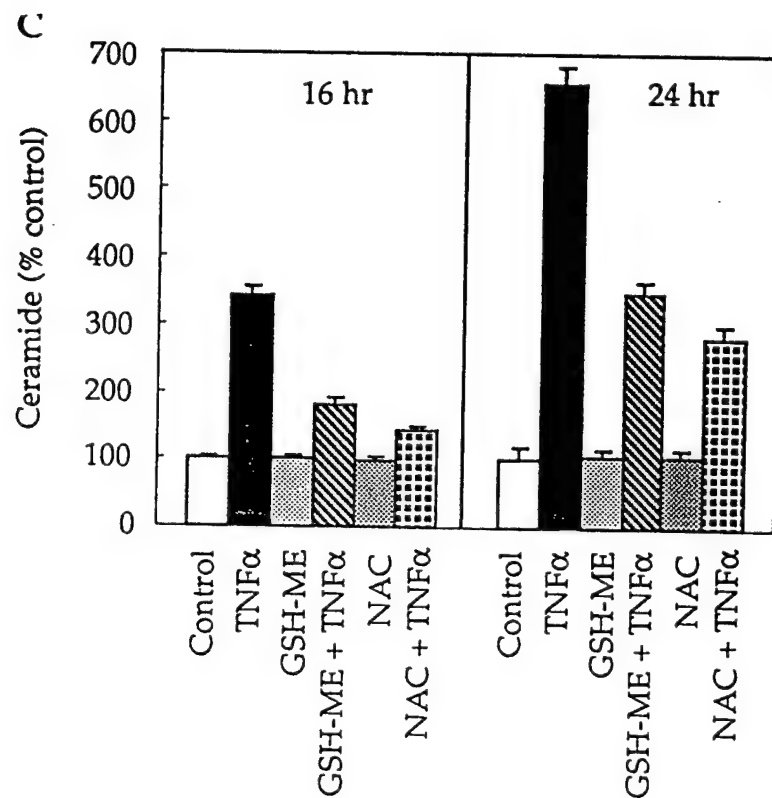


Figure 10C

A

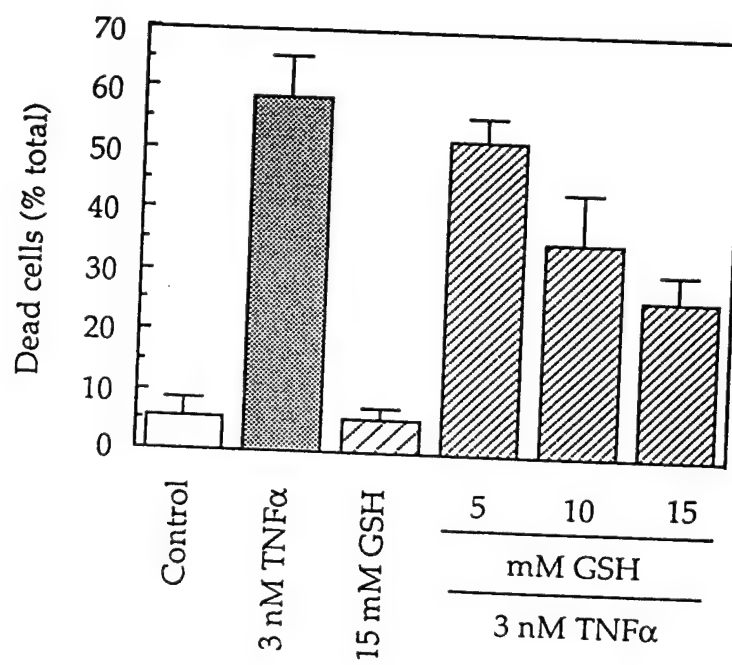


Figure 11A

B

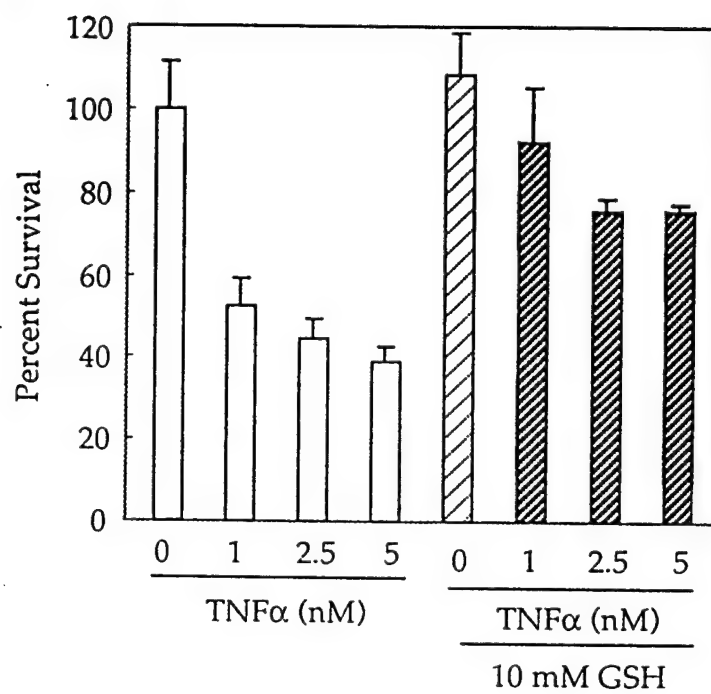


Figure 11B

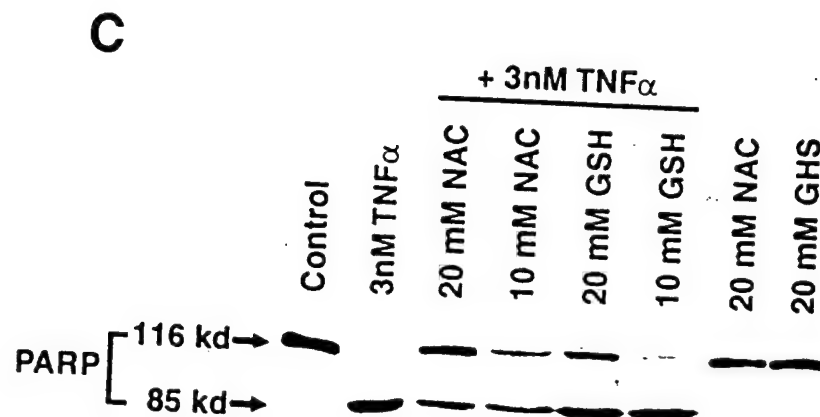


Figure 11C

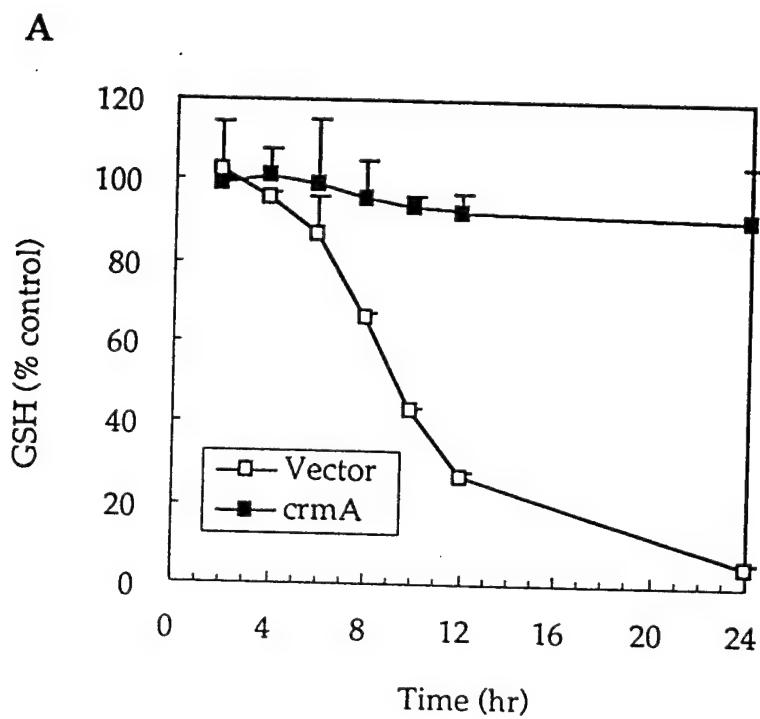


Figure 12A

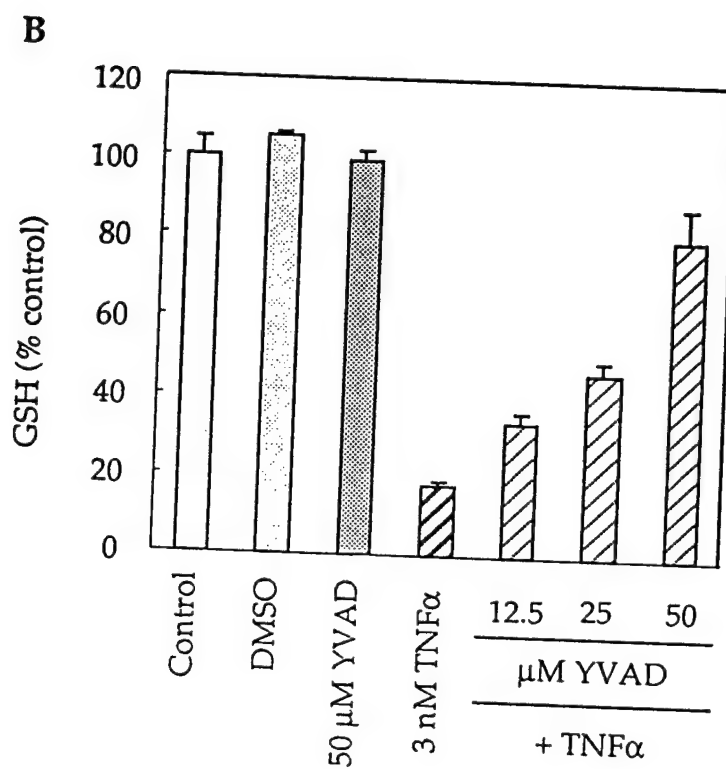


Figure 12B

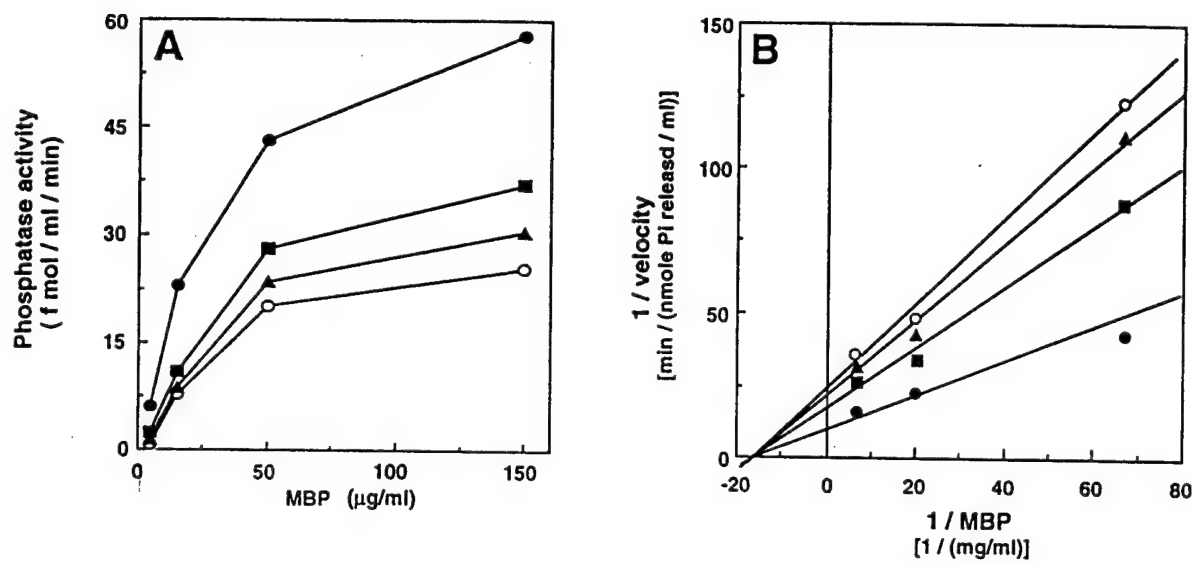


Figure 13

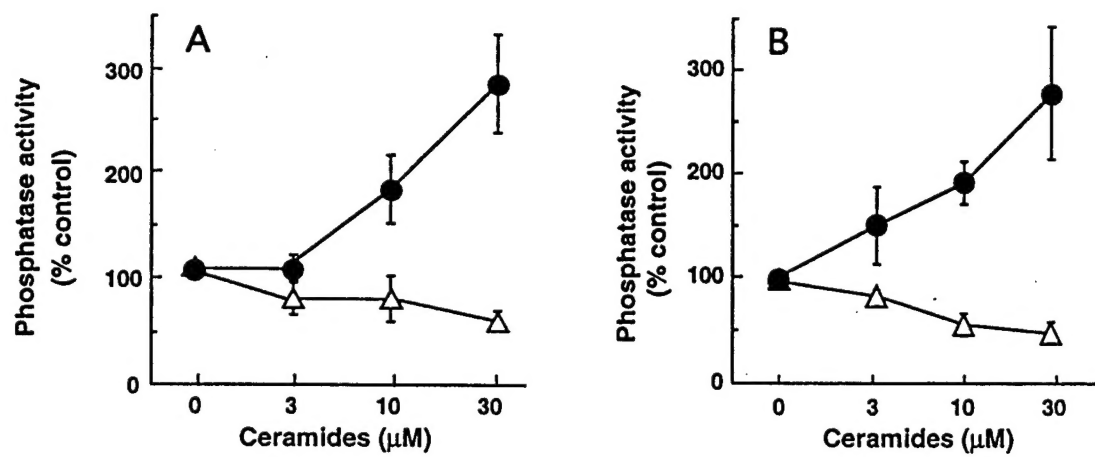


Figure 14

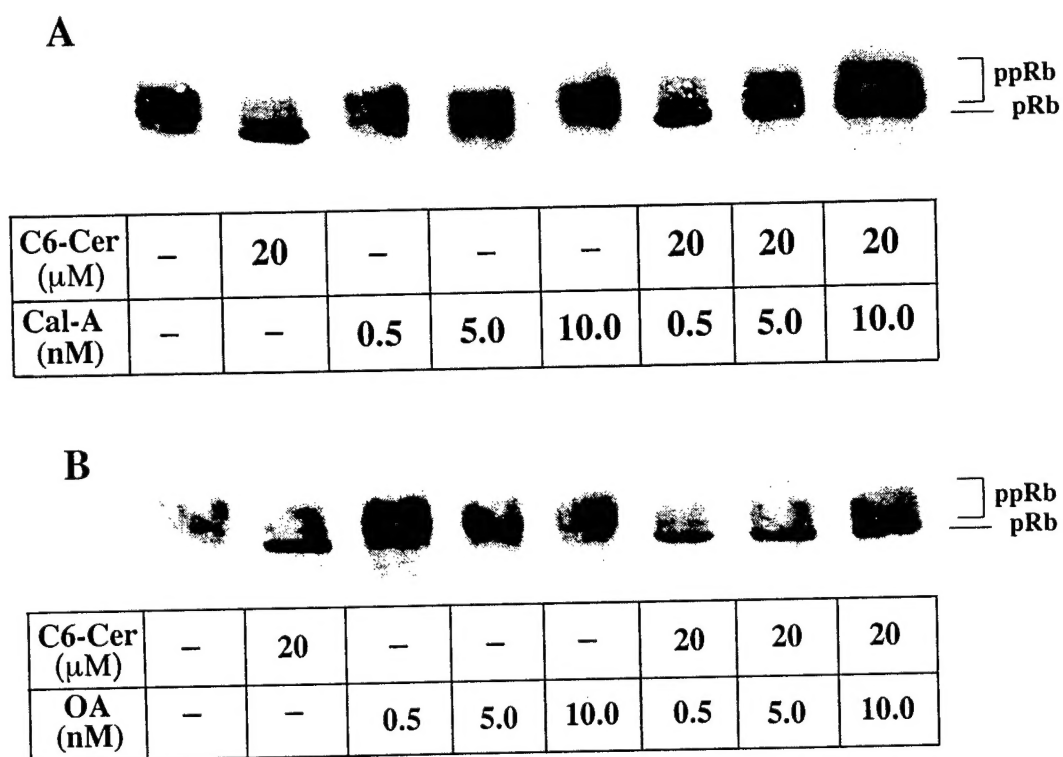


Figure 15

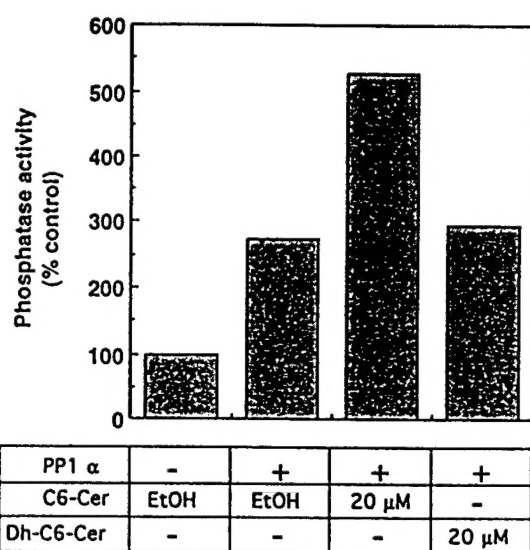


Figure 16

I. Bibliography:

1. Perry, D.K., Smyth, M.J., Wang, H-G., Reed, J.C., Poirier, G.G., Obeid, L.M., and Hannun, Y.A. (1997) Bcl-2 Acts Upstream of the PARP Protease and Prevents Its Activation. *Cell Death and Differentiation* 4, 29-33.
2. Dbaibo, G.S., Perry, D.K., Gamard, C.J., Platt, R., Poirier, G.G., Obeid, L.M., and Hannun, Y.A. (1997) Cytokine Response Modifier A (CrmA) Inhibits Ceramide Formation in Response to Tumor Necrosis Factor (TNF)- α : CrmA and Bcl-2 Target Distinct Components in the Apoptotic Pathway *J. Exp. Med.* 185, 481-490.
3. Hannun, Y.A. (1997) Apoptosis and the dilemma of cancer chemotherapy. *Blood* 89, 1845-1853.
4. Perry, D. K., Smyth, M. J., Stennicke, H.R., Salvesen, G.S., Duriez, P., Poirier, G.G., and Hannun, Y.A. (1997) Zinc is a potent inhibitor of the apoptotic protease, caspase-3: a novel target for zinc in the inhibition of apoptosis. *J. Biol. Chem.* 272, 18530-18533
5. Dbaibo, G. S. and Hannun, Y.A. (1998) Lessons learned from the cowpox crmA gene: a strategically deployed viral weapon. *Clinical Immunology and Immunopathology*. 86:134 140.
6. Liu, B., Andrieu-Abadie, N., Levade, T., Zhang, P., Obeid, L.M., and Hannun, Y.A. (1998) Glutathione regulation of neutral sphingomyelinase in tumor necrosis factor α -induced cell death. *J. Biol. Chem.* 273: 11313-11320.
7. Luberto, C. and Hannun, Y.A. (1998) Sphingomyelin synthase, a potential regulator of intracellular levels of ceramide and diacylglycerol during SV40 trnasformation: does sphingomyelin synthase account for the putative phophatidylcholine-specific phospholipase C? *J. Biol. Chem.* 273: 14550-14559.
8. Dbaibo, G.S., Pushkareva, M.Y., Rachid, R.A., Alter, N., Smyth, M., Obeid, L.M., and Hannun, Y.A. (1998) P53-dependent ceramide response to genotoxic stress. *J.Clin. Invest.* 102: 329-339.

abstract: Y. Hannun: Sphingolipid-mediated apoptosis and tumor suppression in breast carcinoma. presented at the Breast Cancer Research Program: an era of hope; Washington, DC; October 31-November 4, 1997

II. Personnel supported on project:

David Perry
Ghassan Dbaibo
Chiara Luberto
Sandra Merrick